HHS Public Access

Author manuscript

Cell Rep. Author manuscript; available in PMC 2017 July 12.

Published in final edited form as:

Cell Rep. 2016 September 27; 17(1): 289–302. doi:10.1016/j.celrep.2016.08.083.

Reversible Regulation of Promoter and Enhancer Histone Landscape by DNA Methylation in Mouse Embryonic Stem Cells

Andrew D. King[1,2], **Kevin Huang**[1,3], **Liudmilla Rubbi**[4], **Shuo Liu**[5], **Cun-Yu Wang**[3], **Yinsheng Wang**[5], **Matteo Pellegrini**[4], and **Guoping Fan**[1,6]

[1]Department of Human Genetics and Broad Stem Cell Research Center, David Geffen School of Medicine, University of California Los Angeles, Los Angeles, CA 90095, USA

[2]Molecular Biology Interdepartmental Doctoral Program, University of California Los Angeles, Los Angeles, CA 90095, USA

[3]Division of Oral Biology and Medicine, School of Dentistry, University of California Los Angeles, Los Angeles, CA 90095, USA

[4]Department of Molecular, Cell, and Developmental Biology, University of California Los Angeles, Los Angeles, CA 90095, USA

[5]Department of Chemistry, University of California Riverside, Riverside, CA 92521, USA

Summary

DNA methylation is one of a number of modes of epigenetic gene regulation. Here, we profile the DNA methylome, transcriptome, and global occupancy of histone modifications (H3K4me1, H3K4me3, H3K27me3, and H3K27ac) in a series of mouse embryonic stem cells (mESCs) with varying DNA methylation levels to study the effects of DNA methylation on deposition of histone modifications. We find that genome-wide DNA demethylation alters occupancy of histone modifications at both promoters and enhancers. This is reversed upon remethylation by *Dnmt* expression. DNA methylation promotes H3K27me3 deposition at bivalent promoters, while opposing H3K27me3 at silent promoters. DNA methylation also reversibly regulates H3K27ac and H3K27me3 at previously identified tissue-specific enhancers. These effects require DNMT catalytic activity. Collectively, our data show that DNA methylation is essential and instructive for deposition of specific histone modifications across regulatory regions, which together influences gene expression patterns in mESCs.

Graphical abstract

Correspondence to: Guoping Fan.

Lead Contact

Accession Numbers: The accession numbers for the ChIP-seq, RRBS, and RNA-seq data reported in this paper are available in the NCBI GEO: GSE77004.

Supplemental Information: Supplemental Information includes Supplemental Experimental Procedures and five figures and can be found with this article online at http://dx.doi.org/10.1016/j.celrep.2016.08.083.

Author Contributions: A.D.K., K.H., and G.F. conceived the project and designed the experiments. A.D.K. performed the experiments and analyzed data. L.R. prepared RRBS libraries. S.L. performed mass spectrometry studies. C.-Y.W., Y.W., and M.P. helped data interpretation. A.D.K., K.H., and G.F. wrote the manuscript.

King et al. study the reversible effects of DNA methylation on the deposition of histone modifications in mouse ESCs. While having no impact on H3K4me3, DNA demethylation regulates H3K27me3 and H3K27ac at both promoters and enhancers. When *Dnmts* are reintroduced back to a demethylated genome, DNA methylation re-establishes wild-type chromatin states.

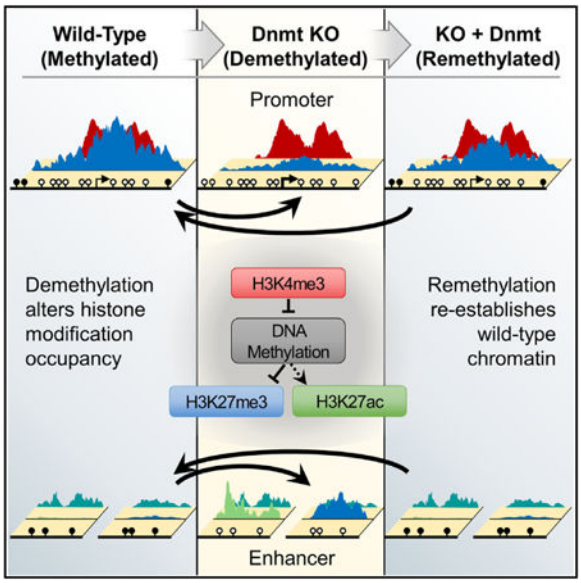

Introduction

Recent studies have revealed that global DNA methylation is dramatically altered during pre- and post-implantation development (Guo et al., 2014; Smith et al., 2014), primordial germ cell reprogramming (Gkountela et al., 2015; Guo et al., 2015b; Tang et al., 2015), as well as stem cell differentiation (Xie et al., 2013) and cellular reprogramming (Lister et al., 2011). A major challenge in the field has been to understand how drastic changes in methylomes contribute to altered transcriptional programs associated with cell-fate commitment and differentiation. The prevailing hypothesis posits that DNA methylation is a crucial silencer of pluripotency and tissue-specific genes via promoter hypermethylation. However, gene promoters account for a tiny fraction of the genome, and increasing evidence repudiates the obligate role for promoter methylation in gene silencing (Bogdanovic et al., 2011; Hammoud et al., 2014; Noh et al., 2015). For instance, pluripotency genes can be silenced during differentiation in the absence of promoter methylation (Sinkkonen et al., 2008). Therefore, it is becoming increasingly clear that DNA methylation works in conjunction with other factors to properly regulate gene expression (Fouse et al., 2008).

DNA methylation and histone modifications are two mediators of epigenetic regulation. These two marks cooperate at many times during development, including silencing of pluripotency genes, genomic imprinting, and X chromosome inactivation (Cedar and Bergman, 2009). Currently, two models describe the relationship between DNA methylation and histone modifications. A number of studies support the idea that DNA methylation is targeted and patterned by histone modifications in the “follower” model, where DNA

methylation acts downstream in the regulatory hierarchy. For example, de novo DNA methyltransferases (DNMT) are shown to recognize unmethylated histone H3 (H3K4me0) at promoters specifying methylation patterns at promoters (Guo et al., 2015a; Ooi et al., 2007; Otani et al., 2009; Zhang et al., 2010). Similarly, H3K36me3 has recently been shown to target DNMT3B to gene bodies contributing to genic methylation (Baubec et al., 2015; Morselli et al., 2015). Alternatively, mounting evidence argues for an instructive role for DNA methylation that regulates histone modification patterns, acting higher in the hierarchy. Under certain circumstances, DNA methylation has been found to be antagonistic to H3K27me3 at promoters. At these sites, methylated DNA is found to exclude binding of PRC2 components to their targets, providing a mechanistic basis for mutual exclusion (Bartke et al., 2010; Jermann et al., 2014). In addition, DNMT3A enzyme was found to facilitate neurogenic gene expression through the exclusion of Polycomb protein binding in gene bodies (Wu et al., 2010). In short, the complex relationship between DNA methylation and histone modifications remains to be illustrated, possibly in a cell-type and/or genomic region-specific manner.

To understand how DNA methylation may coordinate with histone modifications to regulate genome-wide gene expression, we and others have leveraged hypomethylated mouse embryonic stem cells (mESCs), which are viable despite complete loss of genomic DNA methylation. We have previously found that mESCs null of DNA methylation show upregulation of genes primarily associated with bivalent (H3K4me3/H3K27me3 positive) or unmarked (H3K4me3/H3K27me3 double negative) gene promoters in wild-type cells (Fouse et al., 2008). In contrast, minimal changes in H3K9me3 occupancy were observed in hypomethylated mESCs, leading to the idea that DNA methylation and H3K9me3 act non-redundantly (Karimi et al., 2011). Meanwhile, H3K27me3 is dramatically redistributed in response to DNA hypomethylation (Brinkman et al., 2012; Cooper et al., 2014; Reddington et al., 2013). Despite these findings, it is still inconclusive whether the changes of histone modifications observed in DNA methylation null mESCs are directly or indirectly caused by hypomethylation.

In this current study, we set out to understand how DNA methylation shapes the histone landscape and transcriptome in mESCs. To study this, we employed sets of mESC with fully methylated and globally demethylated genomes, or with various intermediate levels of hypomethylation followed by subsequent measurement of histone modifications and RNA transcriptome across all states. Thus, our experimental setup is designed to determine whether DNA methylation acts upstream or downstream with respect to several histone modifications. We show that DNA methylation reversibly regulates occupancy of H3K27me3 and H3K27ac at both gene promoters and tissue-specific enhancer elements. Indeed, changes in H3K27me3 and H3K27ac histone modifications are reversed upon DNMT reconstitution, dependent on DNMT catalytic activity, indicating the ability of DNA methylation to outcompete established chromatin states.

Results

Dnmt Reconstitution in Demethylated mESCs Restores Global Cytosine Methylation and Causes Various Changes in Histone Modifications

To dissect causal relationships between DNA methylation and histone modifications, we simultaneously knocked out all three DNA methyltransferases, *Dnmt1*, *Dnmt3a*, and *Dnmt3b* via Cre-lox recombination to generate triple *Dnmt* knockout (TKO) mouse embryonic stem (ES) cells that are completely devoid of DNA methylation after several cell passages (Figure 1A). By contrast, double knockout (DKO) of the de novo DNA methyltransferases *Dnmt3a* and *Dnmt3b* leads to slower global demethylation (presumably due to the robust *Dnmt1* maintenance enzyme) and reaches 90% loss of global methylation by 30 passages (Jackson et al., 2004) (Figure 1B). In these two demethylated mESC systems, we then reconstituted *Dnmt3a1, Dnmt3a2,* and *Dnmt3b1* isoforms individually (Figures 1A and S1A). Reconstitution of the de novo DNMTs in TKO mESCs resulted in increased global methylation to approximately half of wild-type (WT) levels (Figure 1B). In DKO mESCs, reconstitution of *Dnmt3a1*, *Dnmt3a2,* or *Dnmt3b1* led to a greater increase of methylation to >70% WT levels, indicating a significant contribution from *Dnmt1.* Profiling the DNA methylomes of TKO and DKO reconstitution cell lines using reduced representation bisulfite sequencing (RRBS) showed global levels of cytosine methylation consistent with mass spectrometry results (Figures 1B and S1B). Together, these cell lines enable the study of relationships between varying global methylation levels and histone occupancy.

Mapping average methylation across all genes, we find similar methylation distribution patterns, but different amplitudes proportional to global methylation levels (Figure S1C). Inspection of individual CpG sites revealed that the amplitude differences between cell lines are explained by cytosines being partially methylated rather than a skewed distribution of fully methylated and unmethylated CpGs (Figure S1B). Together, our data suggest that *Dnmt3a* and *Dnmt3b* isoforms are all capable of shaping the overall DNA methylome patterning.

Using chromatin immunoprecipitation sequencing (ChIP-seq), we profiled genomic occupancy of H3K4me3, associated with active promoters, H3K27me3 associated with repressive chromatin, H3K27ac, associated with active promoters and enhancers (Creyghton et al., 2010), and H3K4me1, associated with regulatory regions including enhancers (Barski et al., 2007; Heintzman et al., 2007). Comparison across WT, TKO, DKO, and *Dnmt* reconstitution cell lines reveals selective global changes in specific histone modifications. Genome-wide correlation between all histone modifications and cell lines revealed that correlation generally exists among each histone modification. For example, H3K4me3 across samples are highly correlated (Pearson correlation, $r > 0.96$) (Figure 1C), indicating that H3K4me3 is largely unaffected by global hypomethylation.

Among H3K27ac datasets, inter-sample correlation is also high ($r \sim 0.93$); however, there may be few site-specific differences resulting from hypomethylation. By contrast, H3K27me3 appears to be most sensitive to varying levels of global DNA methylation. WT have 0.63 and 0.65 Pearson correlation with TKO and DKO respectively, >0.7 correlation

with reconstitution in TKO and >0.8 correlation with reconstitution in DKO (Figure 1C, lower-left corner). Correlations are also seen between histone modifications, for example between H3K4me1 and H3K27ac (r ~0.40) and between H3K27me3 and H3K4me3 in WT (r ~0.18), suggesting co-localization in a significant portion of the genome. Epigenetic profiling across mESC lines of different global methylation states is shown at several genomic loci, illustrating histone modification changes sensitive to DNA methylation (Figure 1D). Overall, this indicates a broad role for DNA methylation in influencing histone modifications, with different histone modifications showing different relationships.

DNA Methylation Is Required for Maintenance and Re-establishment of Promoter H3K27me3

As we observed the greatest global variation in H3K27me3 occupancy in response to DNA hypomethylation, we aimed to further investigate the relationship between DNA methylation and H3K27me3 at promoters. We first organized promoters by chromatin environment, categorizing promoters into H3K4me3^{+}, bivalent, H3K27me3^{+}, and silent devoid of both H3K4me3 and H3K27me3 histone modifications (Fouse et al., 2008) (Figure 2A). Consistent with previous studies, we find that H3K27me3 is reduced at nearly all bivalent promoters (3,231/5,362 = 60.3%) in demethylated mESCs (Brinkman et al., 2012; Cooper et al., 2014) (Figures 2A and 2B). The loss of H3K27me3 at bivalent promoters is also associated with a small gain in H3K27ac and loss of H3K4me1 at a subgroup of promoters (Figures S2A–S2C). In contrast, for a subgroup of silent promoters (H3K4me3 and H3K27me3 negative) (705/9,068 = 7.8%), we find increased H3K27me3 occupancy in the demethylated state. For example, promoters of *Cdkn2a* and *Pdgfb* are bivalently marked and upon demethylation and entirely lose H3K27me3 (Figure 2C). In the case of *Cdkn2a*, the promoter is seen to gain H3K27ac. In contrast, *Trpv1*, which is devoid of H3K4me3 and H3K27me3, gains H3K27me3 upon demethylation (Figure 2C). Interestingly, this increase of H3K27me3 extends to adjacent regions including the gene body. Together, these data indicate that DNA methylation is necessary for the maintenance of normal promoter H3K27me3 patterns in a context-specific manner.

We next asked whether DNA methylation can re-establish normal H3K27me3 patterns by reconstituting *Dnmt* in demethylated mESCs. Expression of *Dnmt3a1*, *Dnmt3a2*, and *Dnmt3b1* in TKO and DKO mESCs restores variable levels of H3K27me3 occupancy around promoters (Figures 2A and 2D). At bivalent promoters, *Dnmt3a1* and *Dnmt3a2* appear to have a slightly stronger impact in restoring H3K27me3 compared to *Dnmt3b1*. Nonetheless, neither of the three enzymes alone could fully recapitulate WT patterns when reconstituted in TKO mESCs (Figure S2D). By contrast, reconstitution of *Dnmt3a1*, *Dnmt3a2*, and *Dnmt3b1* in DKO mESCs shows greater H3K27me3 rescue, particularly *Dnmt3a1*, which shows H3K27me3 patterns/levels phenocopying WT(Figures 2A and 2D). Meanwhile, at silent promoters, where demethylation leads to increased levels of H3K27me3 occupancy, we also observe differences in rescue between TKO and DKO reconstitution cell lines. Whereas TKO *Dnmt* reconstitution appears to have weak rescue of H3K27me3 at silent promoter, all *Dnmt* isoforms in DKO are able to restore H3K27me3 down to near WT levels (Figures 2D and S2D). These data show that reconstituted DNMT is capable of re-establishing WT histone modification patterns, indicating DNMT's ability to

outcompete established chromatin states (i.e., the demethylated epigenome) at gene promoters.

Impact of DNA Methylation on Promoter H3K27me3 and Gene Expression Differs between Bivalent and Silent Promoters

To determine the role of DNA methylation in regulation of histone modifications at promoters, we quantified methylation in different categories of promoters (Figure 2E, top). Bivalent promoters are hypomethylated with an average methylation fraction of 0.17, while silent promoters are hypermethylated with an average of 0.88 (Figure 2E). As CpG islands are frequently found at gene promoters and are hypomethylated, we measured the CpG content of promoters in each category, represented as CpG observed-to-expected ratio (CpG O/E). We find bivalent promoters are CpG-rich (O/E >0.6), consistent with the association of bivalent promoters with CpG islands (Bernstein et al., 2006). Silent promoters that gain H3K27me3 are characterized by low CpG content (O/E <0.4), consistent with low CpG-content promoters (LCPs) being predominately methylated in mESCs (Fouse et al., 2008; Weber et al., 2007). Analysis of DNA methylation in KO and reconstitution cell lines shows loss and recovery of WT methylation levels and patterns (Figure 2E, bottom). Bivalent promoters, such as *Cdkn2a* and *Pdgfb*, showed a characteristic hypomethylated CpG island surrounding the transcriptional start site (TSS), while silent promoters, such as *Trpv1*, were heavily methylated (Figures 2C and 2E).

Comparing average H3K27me3 occupancy at transcriptional start sites with global 5mC between cell lines reveals strong associations between DNA methylation and promoter H3K27me3 (Figure 2F). Average H3K27me3 positively correlates with global DNA methylation at bivalent promoters (Pearson correlation, r = 0.84), whereas H3K27me3 is anti-correlated with global DNA methylation at silent promoters (r = 0.95) (Figure 2F). These data suggest a predictive ability of global DNA methylation levels on H3K27me3 occupancy in two promoter contexts.

To test whether alterations in histone modification resulting from demethylation induce any change in gene expression, we profiled the transcriptome from all cell lines. Genes with bivalent promoters generally had low expression (RPKM <10) but significantly increased (mean RPKM increase from 3.9 to 4.8) upon demethylation (Figure 2G). Alternatively, silent promoters were not expressed (RPKM <1) and on average remained silenced despite demethylation. In the case of bivalent promoter gene *Cdkn2a*, we saw gene expression increase over 2-fold in DKO with re-suppression upon remethylation in *Dnmt* reconstitution mESCs.

DNA Methylation Maintains and Re-establishes Silent or Primed States at Enhancer Elements

Differential DNA methylation is prevalent at tissue-specific enhancers (Andersson et al., 2014; Elliott et al., 2015; Hon et al., 2013; Stadler et al., 2011; Thurman et al., 2012; Ziller et al., 2013), suggesting a regulatory role for DNA methylation at enhancer elements. We therefore extended our analysis to enhancers, analyzing H3K27ac/me3 and H3K4me1 modifications (Heintzman et al., 2007). We predicted that genomic hypomethylation would

lead to activation of silent enhancers either as appearance of active enhancers (marked with both H3K27ac and H3K4me1) or as poised enhancers (marked with H3K27me3 and H3K4me1) in TKO (Figure 3A) (Creyghton et al., 2010; Rada-Iglesias et al., 2011; Zentner et al., 2011).

To identify putative methylation-dependent enhancer sites, we identified differentially enriched peaks between demethylated DKO/TKO and their respective methylated wild-type mESCs. Differential peaks were overlapped with H3K4me1 and those within 2 kb of known TSS were excluded to avoid identification of gene promoters. Identifying differential peaks common to both DKO and TKO yielded a number of changes in the chromatin state of candidate enhancers upon genomic hypomethylation (Figure 3A). For example, we observed 138 (1.3%) and 551(5.2%) peaks gaining and losing H3K27ac, respectively. Similarly, we found 1,041 (46.5%) peaks gained and 162 (7.2%) peaks lost H3K27me3 in response to global demethylation. We noted that candidate enhancers that become active or poised in *Dnmt* KO mESCs predominately arise de novo from previously primed enhancer loci in WT mESCs (Figure 3B). Few new active or poised enhancers derive from the other indicating that methylation does not regulate transitions between active and poised status.

We then sought to determine whether or not remethylation would be able to return the enhancers to their original state. If chromatin state takes precedence over DNA methylation, we would expect histone modification status of reconstituted cell lines to resemble the demethylated state. On the other hand, if DNA methylation is capable of acting upstream in the hierarchy, the chromatin state would be reversible. We find that for both H3K27ac and H3K27me3, re-establishing DNA methylation returns putative enhancers to the wild-type state, exemplified by de novo intergenic active enhancer upstream of *Foxd3* as previously characterized in TKO mESCs (Domcke et al., 2015), and an intragenic poised enhancer in *Tmem104* (Figure 3C). The histone modification changes characterized in demethylated DKO and TKO mESCs were uniformly reversible across all enhancers identified (Figures 3D and S3). Similar to rescue at promoters, *Dnmt* reconstitution in DKO more efficiently re-establishes wild-type patterns of enhancers compared to in TKO (Figure 3D).

Enhancers that tend to lose H3K27ac or H3K27me3 are relatively hypomethylated in WT mESCs, whereas enhancers that gain H3K27ac or H3K27me3 are relatively hypermethylated (Figure 3E). This is consistent with antagonism between modifications of the H3K27 residue with DNA methylation (Bartke et al., 2010; Jermann et al., 2014). Measuring CpG content, all enhancers sensitive to DNA methylation consistently show low CpG O/E (O/E <0.4) (Figure 3E). In contrast with CpG-rich bivalent promoters that lose H3K27me3, poised enhancers losing H3K27me3 are low in CpG content.

Lastly, to test whether chromatin state at enhancers alters gene expression, we measured gene expression at both genes nearest to each enhancer (data not shown), as well as a subset of promoters with previously confirmed Hi-C interactions with DNA methylation-sensitive enhancers we identified (Shen et al., 2012). Expression changes at genes associated with methylation-sensitive enhancers varied in their response to demethylation, where each category included genes up- and downregulated (Figure 3F). Median fold change within enhancer categories indicated nearly equal up- and downregulation. However, several genes

exhibit expression patterns indicative of regulation by enhancer methylation. In the case of *Elmo1*, gene expression increased greater than 2-fold in association with a de novo active enhancer within the first intron (Figure 3G). Reconstitution of *Dnmt* also returned both expression of *Elmo1* as well as the intragenic enhancer to wild-type levels. Together, this shows that there are hundreds of enhancers in mESCs where DNA methylation is the primary factor in determining the modification status of chromatin.

De Novo Enhancers Are Tissue Specific and Contain Methylation-Sensitive Transcription Factor Binding Motifs

To characterize DNA methylation-sensitive enhancers, we cross-referenced these enhancers with previously identified tissue-specific enhancers to assess their identity (Shen et al., 2012) (Figure 4A). Of the active enhancers that significantly gain or lose H3K27ac upon DNA demethylation, 33.3% (46/138) and 40.8% (225/551) overlapped with tissue-specific enhancers respectively. In both categories, mESC-specific enhancers were found, with nearly two-thirds of active enhancers losing H3K27ac predictably consisting of mESC-specific enhancers. De novo active enhancers that gained H3K27ac showed overlap with several testes, liver, placenta, and kidney-specific enhancers, with the remainder divided between 14 other tissues (Figure 4A). Both enhancers that gain and lose H3K27me3 also overlapped with tissue-specific enhancers showing 33.2% (346/1,041) and 23.5% (38/162) overlap respectively. Interestingly, de novo poised enhancers overlap with previously identified enhancers from a variety of different tissue types. Meanwhile, enhancers losing H3K27me3 are predominately specific to testes (76%), with a smaller contribution from other tissue types.

To determine how DNA methylation regulates enhancers, we assessed DNA methylation-sensitive enhancers for enrichment of transcription factor motifs. We focused on enhancers gaining H3K27ac or H3K27me3, representing de novo active or poised enhancers, as sites losing these marks are already active/poised and are predictably enriched in pluripotency factors (Figure S4). We find that de novo active enhancers (gain H3K27ac in *Dnmt* KO) are strongly enriched in motifs for NRF1 (16%) and Nkx family transcription factors (87%) (Figure 4B). Interestingly, NRF1 was recently described to be a DNA methylation-dependent transcription factor where methylation of CpG within the binding motif affected binding to DNA (Domcke et al., 2015). In our data, we identified several instances of de novo methylation-dependent active enhancers with underlying methylated NRF1 motifs (Figure 4C). For example, at a testes-specific enhancer upstream of *Zfp92*, we find a DNA methylation-dependent peak with adjacent Nkx2.5 and NRF1 motifs. NRF1 at this enhancer is methylated at an intermediate level (0.29-0.57) in mESCs and is specifically demethylated (<0.05) in adult germline stem cells (AGSCs) of the testis (Hammoud et al., 2014). Similarly, a placenta-specific enhancer is found intragenically in *Ears2*, where a local NRF1 motif is methylated (0.83) in mESCs. The motif for ZBTB33 (also known as Kaiso), a transcriptional regulator described to bind methylated CGCG motif in vitro, was also found at six sites (4.4%).

At de novo poised enhancers (gain H3K27me3 in *Dnmt* KO), we find enrichment of several motifs containing the canonical E box sequence CACGTG as well as motifs for pluripotency

factor Esrrb (Figure 4B). Notably, Myc and Max were also identified as putative methylation-dependent transcription factors (Domcke et al., 2015). Together, these data show that DNA methylation can act upstream of modified H3K27, likely by means of modulating binding of DNA methylation-dependent transcription factors.

Regulation of H3K27me3 Depends on 5-Methylcytosine and DNMT Catalytic Activity

In understanding the relationship between DNA methylation and histone modifications, it is important to distinguish between effects directly conferred by 5-methylcytosine (5mC), DNMT-protein interactions, and other indirect effects. To test whether the methylcytosine moiety of DNA itself or DNMT protein is responsible for re-establishing H3K27me3 at gene promoters, we reconstituted a catalytically null mutant of *Dnmt3b1* (*Dnmt3b1*^{MUT}) that contains missense mutations in the essential PC motif in DKO mESCs. Promoter H3K27me3 in the reconstitution with catalytic mutant resembled DKO at both bivalent and silent promoters. This demonstrates that the ability of DNMT to re-establish H3K27me3 patterns in TKO and DKO mESCs is dependent on DNMT catalytic activity and 5mC (Figures 5A and 5B). Similarly, at poised enhancer elements gaining/losing H3K27me3, *Dnmt3b1*^{MUT} is unable to rescue H3K27me3 redistribution compared to wild-type *Dnmt3b* (Figure 5C). For example, *Dnmt3b1*^{MUT} showed lack of regulation of H3K27me3 at promoters of bivalent *Cdkn2a* and silent *Trpv1*, as well as intragenic de novo poised enhancer in *Tmem104* and intergenic poised enhancer lost upstream of *Foxp4* (Figure 5D). This is consistent with a previous study of *Dnmt3a1* catalytic mutants in neural stem cells, which show an inability to reverse PRC2/H3K27me3 occupancy (Wu et al., 2010).

DNA Methylation Regulation of H3K27me3 Is Mediated by PRC2 Targeting

We have shown that both promoters and enhancers prone to gaining H3K27me3 are heavily methylated in WT, consistent with a direct antagonism between DNA methylation and H3K27me3. To test whether this direct relationship extends to the respective catalytic enzymes, we analyzed published genome binding data of DNMT3A2, DNMT3B1, and SUZ12 (Baubec et al., 2015; Cooper et al., 2014). Similar to measurements of DNA methylation profiles at promoters and enhancers, we find that DNMT3A2 and DNMT3B1 are preferentially bound to silent promoters and de novo poised enhancers that both gain H3K27me3 in TKO (Figures 6A and 6B). Likewise, SUZ12 binding mirrors H3K27me3 occupancy, where SUZ12 binding increases at silent promoters in TKO (Cooper et al., 2014). In a similar manner, SUZ12 increases strongly at de novo poised enhancers (Figures 6A and 6B). The strong presence of DNMT and 5mC at silent promoters and de novo poised enhancers that gain SUZ12 and H3K27me3 upon demethylation suggests direct antagonism between DNA methylation and PRC2 complex as previously described in neural progenitor cells (NPCs) (Wu et al., 2010). In contrast, bivalent promoters are unmethylated and lack DNMT binding, implying an indirect mechanism for regulating H3K27me3 and PRC2.

Differences of *Dnmt3a* and *Dnmt3b* Isoforms in Histone Modification Regulation

For the two catalytically active de novo methyltransferases, multiple isoforms have been characterized. These isoforms are expressed in a tissue and developmentally regulated manner. In mESCs, *Dnmt3a2* and *Dnmt3b1* are the major isoforms, while *Dnmt3a1* is expressed at a lower level and increases in expression throughout development (Chen et al.,

2002; Feng et al., 2005). Methylation patterns are determined through differential expression of *Dnmt3a* and *Dnmt3b* isoforms (Chen et al., 2003) but are redundant as certain targets, such as *Oct4* and *Nanog*, are still able to be methylated in single knockouts (Li et al., 2007). We therefore asked whether different *Dnmt3* isoforms have unique or shared targets across the genome. Segmenting the genome into 500 bp windows, we found that the vast majority of methylated windows (26M bases) can be methylated by all three isoforms (90%). Interestingly, we identify a tiny fraction of the genome (in total about 200 kb or <1%) that appear either *Dnmt3a1* specific, *Dnmt3a2* specific, or *Dnmt3b1* specific. Therefore, the three *Dnmt3* isoforms have highly redundant genomic targets.

We next evaluated the effect on histone modifications by different *Dnmt* isoforms. One challenge in measuring these differences is the inherent lack of quantitative ability of conventional ChIP-seq, precluding accurate and quantitative comparison between isoforms. We therefore compared histone modifications between *Dnmt* reconstitution lines and performed comparison with reference to background to account for systematic differences between ChIP-seq libraries. We find that all *Dnmt* isoforms studied were able to regulate H3K27me3 and re-establish WT patterns to some extent at promoters, indicating redundancy in their function. This is also evident in the ability of *Dnmt* isoforms to re-establish similar global methylation levels (Figure 1B). However, of the three enzymes, *Dnmt3b1* reconstitution showed the least recapitulation toward WT despite similar ability to remethylate the genome. Measuring the ratio of H3K27me3 occupancy between *Dnmt3* isoforms at bivalent promoters, we find that *Dnmt3a1* and *Dnmt3a2* restore H3K27me3 to higher levels than *Dnmt3b1* (Figures S5A and S5B). Similarly, at silent promoters, both *Dnmt3a2* and *Dnmt3a1* resuppress H3K27me3 to a greater extent than *Dnmt3b1* (Figures 2D, S5A, and S5B).

At enhancers, we found *Dnmt3a1* and *Dnmt3a2* show greater recovery of H3K27me3 at poised enhancers losing H3K27me3 and greater resuppression of H3K27me3 at de novo poised enhancers than *Dnmt3b1* (Figures S5C and S5D). Likewise, comparison of H3K27ac changes between reconstitution lines showed that both *Dnmt3a2* and *Dnmt3a1* restored WT patterns more than *Dnmt3b1* (Figure S5E). Overall, these comparisons indicate a potential bias between *Dnmt3a* and *Dnmt3b* in the regulation of histone modifications at promoters and enhancer elements.

Discussion

In the current study, we combined sequential genetic alteration of DNA methylation levels with systematic and comprehensive mapping of histone modifications to assess how DNA methylation influences the epigenomic and transcriptomic landscape. Our experiments show the active histone modification H3K4me3 is deposited independently of DNA methylation, while DNA methylation acts upstream of H3K27me3, H3K27ac, and H3K4me1, which have regulatory consequences at both gene promoters and enhancers. Another key finding in our study was the reversibility of the histone landscape in response to demethylation and newly established methylcytosine marks (Figure 7). Thus, DNA methylation is situated within a hierarchy of epigenetic regulation where it is required for regulation of some histone modifications.

Measurement of histone modifications showed different responses to genome-wide demethylation. For example, H3K4me3 did not change in response to global hypomethylation. This is in contrast to somatic cells, where hypomethylation results in appearance of new H3K4me3 peaks, albeit far fewer than H3K27me3 (Reddington et al., 2013). This indicates that DNMT acts downstream of H3K4me3 in ESCs. The downstream position of DNA methylation is consistent with mechanistic studies of de novo methylation showing exclusion of DNMT binding to sites marked with H3K4me3 (Noh et al., 2015; Ooi et al., 2007; Otani et al., 2009; Zhang et al., 2010). H3K4me1 on the other hand showed moderate changes at promoters in *Dnmt* KO indicating sensitivity to DNA methylation. Binding affinity of H3K4me1 to DNMT3A-ADD and DNMT3L was over an order of magnitude greater than H3K4me3, indicating methylation states of H3K4 differ in their relationship with DNA methylation (Noh et al., 2015; Ooi et al., 2007). H3K4me3 therefore belongs to a list of histone modifications including H3K9me3 and H3K36me3 that dictate DNMT localization in ESCs.

One model for the relationship between H3K27me3 and DNA methylation is that EZH2 targets DNMT for de novo methylation. The preferential de novo methylation at Polycomb targets in many cancers lends credence to this notion (Gal-Yam et al., 2008). EZH2 and DNMT1/3A/3B were shown to physically interact, where EZH2 is required for DNMT binding at EZH2 targets in HeLa cells (Viré et al., 2006). Based on this model, DNMTs would not influence H3K27me3 as PRC2 acts upstream of DNMT. However, in contrast to this model, we find that loss of DNA methylation affects the maintenance of H3K27me3 patterns, which are then able to be re-established with DNMT reconstitution, indicating that DNA methylation functionally acts upstream of PRC2 activity in mESCs. DNA methylation acting upstream of histone modifications is not unprecedented, where DNA methylation has been shown to target H3K9 methyl-transferase activity in fibroblasts (Fuks et al., 2003). Recently, DNA methylation was found to recruit SETDB1 and consequently H3K9me3 to key developmental genes in preadipocytes (Matsumura et al., 2015). However, in ESCs, DNA methylation is not required for H3K9me3 deposition (Karimi et al., 2011). These differences could be due to intrinsic differences between embryonic and somatic cells or particular cell states.

We found that the relationship between global DNA methylation and H3K27me3 is dependent on genomic context. The negative correlation at silent promoter is consistent with the antagonism between DNA methylation and H3K27me3 (Bartke et al., 2010; Fouse et al., 2008; Mikkelsen et al., 2007). However, the positive correlation at bivalent promoters is unexplained. Bivalent promoters are unmethylated precluding a direct influence of methylcytosine on PRC2 at these sites. The leading thought is that antagonism between DNA methylation and PRC2 constrains H3K27me3 within CpG islands, which is lost in TKO cells (Brinkman et al., 2012; Reddington et al., 2013). In this case, in cells lacking DNA methylation, H3K27me3 is aberrantly deposited to regions normally restricted by DNA methylation, resulting in depletion of H3K27me3 at sites such as bivalent promoters. In other words, DNA demethylated regions act as a sink for PcG activity. Alternatively, PRC2 has been shown to bind as a default state to CpG-rich DNA, while being obstructed by active gene expression (Jermann et al., 2014; Riising et al., 2014). DNA methylation could therefore influence gene expression of bivalent genes and consequently regulate H3K27me3.

The order of events between PRC2 binding and gene activity are not yet known, preventing evaluation of such a mechanism. It remains of great interest mechanistically how DNA methylation regulates H3K27me3 at bivalent promoters.

The relationship between DNA methylation and chromatin state at enhancers has largely been based on association, with little indication of order of events (Andersson et al., 2014; Elliott et al., 2015; Hon et al., 2013; Ziller et al., 2013). Our data showing de novo gain of H3K27me3 and H3K27ac at enhancers upon demethylation demonstrate DNA methylation's regulation of chromatin state. This is in agreement with previous work showing loss of H3K27ac resulting from hypermethylation by *Tet2* knockout (Hon et al., 2014; Lu et al., 2014). Notably, our findings showed reversibility of H3K27me3 and H3K27ac changes at both promoters and enhancers. This indicates that DNA methylation can establish silent chromatin states, even over preexisting active states.

At de novo active enhancers, DNA methylation most likely regulates H3K27ac at active enhancers through modulation of transcription factor binding. Recent results showed DNA methylation competes with binding of transcription factor NRF1, where changes in NRF1 binding were reversible between 2i and Serum conditions (Domcke et al., 2015). We identified the NRF1 binding motif enriched at methylation-sensitive active enhancers, indicating regulation of “settler” transcription factor binding as a target of regulation by DNA methylation. We also identified motifs for Kaiso, a factor that binds methylated CpG in vitro and recruits deacetylation complex NCoR to repress gene expression (Yoon et al., 2003). The huge diversity in transcription factors and their individual relationships with DNA methylation represent many potential mechanisms underlying methylation-dependent changes in histone modifications. Several models describing the relationship between DNA methylation and transcription factors have been previously reviewed (Blattler and Farnham, 2013).

Similarly, poised enhancers showed reversible regulation by DNA methylation. Studies support the idea that the three-dimensional architecture of the genome is structured into dense polycomb interfaces (so-called polycomb bodies), providing evidence of higher-order interactions among H3K27me3 enriched sites (Joshi et al., 2015; Li et al., 2015; Wani et al., 2016). It remains to be seen whether DNA methylation can control higher-order interactions via regulation of histone modifications and other structural proteins.

Another question in the field that lacks understanding is what differences exist between *Dnmt* isoforms. Early evidence suggested strong redundancy between isoforms in ESCs as single gene knockouts of either *Dnmt3a* or *Dnmt3b* showed minimal changes in DNA methylation (Chen et al., 2003; Okano et al., 1999). Knockdown of *Dnmt* isoforms revealed hypermethylation of highly transcribed gene bodies upon *Dnmt3b* knockdown, whereas *Dnmt3a* knockdown resulted in global hypomethylation (Tiedemann et al., 2014). DNMT3B was also found to selectively localize to gene bodies of highly transcribed genes through H3K36me3, while DNMT3A showed decreased methylation of highly transcribed genes (Baubec et al., 2015). In our results, we find a dominant role for *Dnmt3a* isoforms over *Dnmt3b* in re-establishing H3K27me3 patterns at both promoters and enhancers. This

provides some clues that differential expression of *Dnmt* isoforms may play a role in regulating chromatin state and gene expression, but much still remains to be studied.

In sum, this research provides a comprehensive resource toward the understanding of how alterations in DNA methylation sculpt the rest of the epigenome. Our results present a model where DNA methylation plays an active role in establishing chromatin states in addition to its classic role in gene silencing via promoter CpG methylation. Thus, in the cascade of epigenetic gene regulation, DNA methylation serves as a multifaceted regulator, acting on both DNA and chromatin in the mammalian genome.

Experimental Procedures

ESC Culture

Mouse embryonic stem cells (mESCs) were grown on irradiated mouse embryonic fibroblasts (MEFs) and maintained in DMEM (Corning) supplemented with 15% fetal bovine serum, 1 mM GlutaMAX (Life Technologies), 1 × non-essential amino acids (NEAA), 1 × penicillin/streptomycin (Life Technologies), mLIF, and 0.001% â-mercaptoethanol (Sigma-Aldrich).

ChIP-Seq and Analysis

ChIP-seq libraries were constructed using Kapa Library Preparation Kit for Illumina sequencing (Kapa Biosystems). Libraries were pooled and sequenced using the Illumina HiSeq machine as either 50 or 100-bp single-end sequencing reads. Sequenced reads were mapped to mouse genome (mm9) using bowtie 1.1.0 allowing up to two mismatches and only unique alignments. Mapped reads were processed using Homer tool suite (Heinz et al., 2010). For details, see the Supplemental Experimental Procedures.

Reduced Representation Bisulfite Sequencing and Analysis

Genomic DNA was purified from mESCs using standard phenol-chloroform-isoamyl alcohol extraction followed by ethanol precipitation. Libraries were generated as previously described with minor modification (Meissner et al., 2005). Libraries were pooled and sequenced using the Illumina HiSeq machine as 100-bp single-end sequencing reads. Reads were mapped to the mouse genome (mm9) with Bismark (Krueger and Andrews, 2011). For details, see the Supplemental Experimental Procedures.

RNA-Seq and Analysis

Total RNA was purified using RNeasy Mini Kit (QIAGEN). Poly(A)-tailed RNA was purified from total RNA and libraries were constructed using the TruSeq RNA Library Prep Kit v.2.0 (Illumina). Libraries were pooled and sequenced using the Illumina HiSeq machine as 100-bp single-end sequencing reads. Reads were mapped to the mouse genome (mm9) with STAR aligner (Dobin et al., 2013). For details, see the Supplemental Experimental Procedures.

Supplementary Material

Refer to Web version on PubMed Central for supplementary material.

Acknowledgments

We thank members of G.F.'s lab for helpful discussion. We thank Suhua Feng and Shawn Cokus at the UCLA Broad Stem Cell Center High Throughput Sequencing Core. We thank Cesar Barragan, Joseph Nery, and Manoj Hariharan at the Salk Center of Excellence in Stem Cell Genomics. This work is supported by the National Institute of Dental and Craniofacial Research (5R21DE022928 and R01DE025474) and a grant from the California Institute for Regenerative Medicine (CIRM) Center of Excellence for Stem Cell Genomics (GC1R-06673-A). A.D.K. is supported by the Eli and Edythe Broad Center of Regenerative Medicine and Stem Cell Research at UCLA Training Program. K.H. is supported by a National Institute of Arthritis and Musculoskeletal and Skin Diseases training grant (T32AR059033).

References

Andersson R, Gebhard C, Miguel-Escalada I, Hoof I, Bornholdt J, Boyd M, Chen Y, Zhao X, Schmidl C, Suzuki T, et al. An atlas of active enhancers across human cell types and tissues. Nature. 2014; 507:455–461. [PubMed: 24670763]

Barski A, Cuddapah S, Cui K, Roh TY, Schones DE, Wang Z, Wei G, Chepelev I, Zhao K. High-resolution profiling of histone methylations in the human genome. Cell. 2007; 129:823–837. [PubMed: 17512414]

Bartke T, Vermeulen M, Xhemalce B, Robson SC, Mann M, Kouzarides T. Nucleosome-interacting proteins regulated by DNA and histone methylation. Cell. 2010; 143:470–484. [PubMed: 21029866]

Baubec T, Colombo DF, Wirbelauer C, Schmidt J, Burger L, Krebs AR, Akalin A, Schübeler D. Genomic profiling of DNA methyltransferases reveals a role for DNMT3B in genic methylation. Nature. 2015; 520:243–247. [PubMed: 25607372]

Bernstein BE, Mikkelsen TS, Xie X, Kamal M, Huebert DJ, Cuff J, Fry B, Meissner A, Wernig M, Plath K, et al. A bivalent chromatin structure marks key developmental genes in embryonic stem cells. Cell. 2006; 125:315–326. [PubMed: 16630819]

Blattler A, Farnham PJ. Cross-talk between site-specific transcription factors and DNA methylation states. J Biol Chem. 2013; 288:34287–34294. [PubMed: 24151070]

Bogdanovic O, Long SW, van Heeringen SJ, Brinkman AB, Gómez-Skarmeta JL, Stunnenberg HG, Jones PL, Veenstra GJC. Temporal uncoupling of the DNA methylome and transcriptional repression during embryogenesis. Genome Res. 2011; 21:1313–1327. [PubMed: 21636662]

Brinkman AB, Gu H, Bartels SJJ, Zhang Y, Matarese F, Simmer F, Marks H, Bock C, Gnirke A, Meissner A, Stunnenberg HG. Sequential ChIP-bisulfite sequencing enables direct genome-scale investigation of chromatin and DNA methylation cross-talk. Genome Res. 2012; 22:1128–1138. [PubMed: 22466170]

Cedar H, Bergman Y. Linking DNA methylation and histone modification: patterns and paradigms. Nat Rev Genet. 2009; 10:295–304. [PubMed: 19308066]

Chen T, Ueda Y, Xie S, Li E. A novel Dnmt3a isoform produced from an alternative promoter localizes to euchromatin and its expression correlates with active de novo methylation. J Biol Chem. 2002; 277:38746–38754. [PubMed: 12138111]

Chen T, Ueda Y, Dodge JE, Wang Z, Li E. Establishment and maintenance of genomic methylation patterns in mouse embryonic stem cells by Dnmt3a and Dnmt3b. Mol Cell Biol. 2003; 23:5594–5605. [PubMed: 12897133]

Cooper S, Dienstbier M, Hassan R, Schermelleh L, Sharif J, Blackledge NP, De Marco V, Elderkin S, Koseki H, Klose R, et al. Targeting polycomb to pericentric heterochromatin in embryonic stem cells reveals a role for H2AK119u1 in PRC2 recruitment. Cell Rep. 2014; 7:1456–1470. [PubMed: 24857660]

Creyghton MP, Cheng AW, Welstead GG, Kooistra T, Carey BW, Steine EJ, Hanna J, Lodato MA, Frampton GM, Sharp PA, et al. Histone H3K27ac separates active from poised enhancers and

predicts developmental state. Proc Natl Acad Sci USA. 2010; 107:21931–21936. [PubMed: 21106759]

Dobin A, Davis CA, Schlesinger F, Drenkow J, Zaleski C, Jha S, Batut P, Chaisson M, Gingeras TR. STAR:ultrafast universal RNA-seq aligner. Bioinformatics. 2013; 29:15–21. [PubMed: 23104886]

Domcke S, Bardet AF, Adrian Ginno P, Hartl D, Burger L, Schübeler D. Competition between DNA methylation and transcription factors determines binding of NRF1. Nature. 2015; 528:575–579. [PubMed: 26675734]

Elliott G, Hong C, Xing X, Zhou X, Li D, Coarfa C, Bell RJA, Maire CL, Ligon KL, Sigaroudinia M, et al. Intermediate DNA methylation is a conserved signature of genome regulation. Nat Commun. 2015; 6:6363. [PubMed: 25691127]

Feng J, Chang H, Li E, Fan G. Dynamic expression of de novo DNA methyltransferases Dnmt3a and Dnmt3b in the central nervous system. J Neurosci Res. 2005; 79:734–746. [PubMed: 15672446]

Fouse SD, Shen Y, Pellegrini M, Cole S, Meissner A, Van Neste L, Jaenisch R, Fan G. Promoter CpG methylation contributes to ES cell gene regulation in parallel with Oct4/Nanog, PcG complex, and histone H3 K4/K27 trimethylation. Cell Stem Cell. 2008; 2:160–169. [PubMed: 18371437]

Fuks F, Hurd PJ, Wolf D, Nan X, Bird AP, Kouzarides T. The methyl-CpG-binding protein MeCP2 links DNA methylation to histone methylation. J Biol Chem. 2003; 278:4035–4040. [PubMed: 12427740]

Gal-Yam EN, Egger G, Iniguez L, Holster H, Einarsson S, Zhang X, Lin JC, Liang G, Jones PA, Tanay A. Frequent switching of Poly-comb repressive marks and DNA hypermethylation in the PC3 prostate cancer cell line. Proc Natl Acad Sci USA. 2008; 105:12979–12984. [PubMed: 18753622]

Gkountela S, Zhang KX, Shafiq TA, Liao WW, Hargan-Calvopiña J, Chen PY, Clark AT. DNA demethylation dynamics in the human prenatal germline. Cell. 2015; 161:1425–1436. [PubMed: 26004067]

Guo H, Zhu P, Yan L, Li R, Hu B, Lian Y, Yan J, Ren X, Lin S, Li J, et al. The DNA methylation landscape of human early embryos. Nature. 2014; 511:606–610. [PubMed: 25079557]

Guo X, Wang L, Li J, Ding Z, Xiao J, Yin X, He S, Shi P, Dong L, Li G, et al. Structural insight into autoinhibition and histone H3-induced activation of DNMT3A. Nature. 2015a; 517:640–644. [PubMed: 25383530]

Guo F, Yan L, Guo H, Li L, Hu B, Zhao Y, Yong J, Hu Y, Wang X, Wei Y, et al. The transcriptome and DNA methylome landscapes of human primordial germ cells. Cell. 2015b; 161:1437–1452. [PubMed: 26046443]

Hammoud SS, Low DHP, Yi C, Carrell DT, Guccione E, Cairns BR. Chromatin and transcription transitions of mammalian adult germ-line stem cells and spermatogenesis. Cell Stem Cell. 2014; 15:239–253. [PubMed: 24835570]

Heintzman ND, Stuart RK, Hon G, Fu Y, Ching CW, Hawkins RD, Barrera LO, Van Calcar S, Qu C, Ching KA, et al. Distinct and predictive chromatin signatures of transcriptional promoters and enhancers in the human genome. Nat Genet. 2007; 39:311–318. [PubMed: 17277777]

Heinz S, Benner C, Spann N, Bertolino E, Lin YC, Laslo P, Cheng JX, Murre C, Singh H, Glass CK. Simple combinations of lineage-determining transcription factors prime cis-regulatory elements required for macrophage and B cell identities. Mol Cell. 2010; 38:576–589. [PubMed: 20513432]

Hon GC, Rajagopal N, Shen Y, McCleary DF, Yue F, Dang MD, Ren B. Epigenetic memory at embryonic enhancers identified in DNA methylation maps from adult mouse tissues. Nat Genet. 2013; 45:1198–1206. [PubMed: 23995138]

Hon GC, Song CX, Du T, Jin F, Selvaraj S, Lee AY, Yen CA, Ye Z, Mao SQ, Wang BA, et al. 5mC oxidation by Tet2 modulates enhancer activity and timing of transcriptome reprogramming during differentiation. Mol Cell. 2014; 56:286–297. [PubMed: 25263596]

Jackson M, Krassowska A, Gilbert N, Chevassut T, Forrester L, Ansell J, Ramsahoye B. Severe global DNA hypomethylation blocks differentiation and induces histone hyperacetylation in embryonic stem cells. Mol Cell Biol. 2004; 24:8862–8871. [PubMed: 15456861]

Jermann P, Hoerner L, Burger L, Schübeler D. Short sequences can efficiently recruit histone H3 lysine 27 trimethylation in the absence of enhancer activity and DNA methylation. Proc Natl Acad Sci USA. 2014; 111:E3415–E3421. [PubMed: 25092339]

Joshi O, Wang SY, Kuznetsova T, Atlasi Y, Peng T, Fabre PJ, Habibi E, Shaik J, Saeed S, Handoko L, et al. Dynamic reorganization of extremely long-range promoter-promoter interactions between two states of pluripotency. Cell Stem Cell. 2015; 17:748–757. [PubMed: 26637943]

Karimi MM, Goyal P, Maksakova IA, Bilenky M, Leung D, Tang JX, Shinkai Y, Mager DL, Jones S, Hirst M, Lorincz MC. DNA methylation and SETDB1/H3K9me3 regulate predominantly distinct sets of genes, retroelements, and chimeric transcripts in mESCs. Cell Stem Cell. 2011; 8:676–687. [PubMed: 21624812]

Krueger F, Andrews SR. Bismark: a flexible aligner and methylation caller for Bisulfite-Seq applications. Bioinformatics. 2011; 27:1571–1572. [PubMed: 21493656]

Li JY, Pu MT, Hirasawa R, Li BZ, Huang YN, Zeng R, Jing NH, Chen T, Li E, Sasaki H, Xu GL. Synergistic function of DNA methyltransferases Dnmt3a and Dnmt3b in the methylation of Oct4 and Nanog. Mol Cell Biol. 2007; 27:8748–8759. [PubMed: 17938196]

Li L, Lyu X, Hou C, Takenaka N, Nguyen HQ, Ong CT, Cubeñas-Potts C, Hu M, Lei EP, Bosco G, et al. Widespread rearrangement of 3D chromatin organization underlies polycomb-mediated stress-induced silencing. Mol Cell. 2015; 58:216–231. [PubMed: 25818644]

Lister R, Pelizzola M, Kida YS, Hawkins RD, Nery JR, Hon G, Antosie-wicz-Bourget J, O'Malley R, Castanon R, Klugman S, et al. Hot-spots of aberrant epigenomic reprogramming in human induced pluripotent stem cells. Nature. 2011; 471:68–73. [PubMed: 21289626]

Lu F, Liu Y, Jiang L, Yamaguchi S, Zhang Y. Role of Tet proteins in enhancer activity and telomere elongation. Genes Dev. 2014; 28:2103–2119. [PubMed: 25223896]

Matsumura Y, Nakaki R, Inagaki T, Yoshida A, Kano Y, Kimura H, Tanaka T, Tsutsumi S, Nakao M, Doi T, et al. H3K4/H3K9me3 bivalent chromatin domains targeted by lineage-specific dna methylation pauses adipocyte differentiation. Mol Cell. 2015; 60:584–596. [PubMed: 26590716]

Meissner A, Gnirke A, Bell GW, Ramsahoye B, Lander ES, Jaenisch R. Reduced representation bisulfite sequencing for comparative high-resolution DNA methylation analysis. Nucleic Acids Res. 2005; 33:5868–5877. [PubMed: 16224102]

Mikkelsen TS, Ku M, Jaffe DB, Issac B, Lieberman E, Giannoukos G, Alvarez P, Brockman W, Kim TK, Koche RP, et al. Genome-wide maps of chromatin state in pluripotent and lineage-committed cells. Nature. 2007; 448:553–560. [PubMed: 17603471]

Morselli M, Pastor WA, Montanini B, Nee K, Ferrari R, Fu K, Bonora G, Rubbi L, Clark AT, Ottonello S, et al. In vivo targeting of de novo DNA methylation by histone modifications in yeast and mouse. eLife. 2015; 4:e06205. [PubMed: 25848745]

Noh KM, Wang H, Kim HR, Wenderski W, Fang F, Li CH, Dewell S, Hughes SH, Melnick AM, Patel DJ, et al. Engineering of a histone-recognition domain in Dnmt3a alters the epigenetic landscape and phenotypic features of mouse ESCs. Mol Cell. 2015; 59:89–103. [PubMed: 26073541]

Okano M, Bell DW, Haber DA, Li E. DNA methyltransferases Dnmt3a and Dnmt3b are essential for de novo methylation and mammalian development. Cell. 1999; 99:247–257. [PubMed: 10555141]

Ooi SKT, Qiu C, Bernstein E, Li K, Jia D, Yang Z, Erdjument-Bromage H, Tempst P, Lin SP, Allis CD, et al. DNMT3L connects unmethylated lysine 4 of histone H3 to de novo methylation of DNA. Nature. 2007; 448:714–717. [PubMed: 17687327]

Otani J, Nankumo T, Arita K, Inamoto S, Ariyoshi M, Shirakawa M. Structural basis for recognition of H3K4 methylation status by the DNA methyltransferase 3A ATRX-DNMT3-DNMT3L domain. EMBO Rep. 2009; 10:1235–1241. [PubMed: 19834512]

Rada-Iglesias A, Bajpai R, Swigut T, Brugmann SA, Flynn RA, Wysocka J. A unique chromatin signature uncovers early developmental enhancers in humans. Nature. 2011; 470:279–283. [PubMed: 21160473]

Reddington JP, Perricone SM, Nestor CE, Reichmann J, Youngson NA, Suzuki M, Reinhardt D, Dunican DS, Prendergast JG, Mjoseng H, et al. Redistribution of H3K27me3 upon DNA hypomethylation results in de-repression of Polycomb target genes. Genome Biol. 2013; 14:R25. [PubMed: 23531360]

Riising EM, Comet I, Leblanc B, Wu X, Johansen JV, Helin K. Gene silencing triggers polycomb repressive complex 2 recruitment to CpG islands genome wide. Mol Cell. 2014; 55:347–360. [PubMed: 24999238]

Shen Y, Yue F, McCleary DF, Ye Z, Edsall L, Kuan S, Wagner U, Dixon J, Lee L, Lobanenkov VV, Ren B. A map of the cis-regulatory sequences in the mouse genome. Nature. 2012; 488:116–120. [PubMed: 22763441]

Sinkkonen L, Hugenschmidt T, Berninger P, Gaidatzis D, Mohn F, Artus-Revel CG, Zavolan M, Svoboda P, Filipowicz W. MicroRNAs control de novo DNA methylation through regulation of transcriptional repressors in mouse embryonic stem cells. Nat Struct Mol Biol. 2008; 15:259–267. [PubMed: 18311153]

Smith ZD, Chan MM, Humm KC, Karnik R, Mekhoubad S, Regev A, Eggan K, Meissner A. DNA methylation dynamics of the human preimplantation embryo. Nature. 2014; 511:611–615. [PubMed: 25079558]

Stadler MB, Murr R, Burger L, Ivanek R, Lienert F, Schöler A, van Nimwegen E, Wirbelauer C, Oakeley EJ, Gaidatzis D, et al. DNA-binding factors shape the mouse methylome at distal regulatory regions. Nature. 2011; 480:490–495. [PubMed: 22170606]

Tang WWC, Dietmann S, Irie N, Leitch HG, Floros VI, Bradshaw CR, Hackett JA, Chinnery PF, Surani MA. A unique gene regulatory network resets the human germline epigenome for development. Cell. 2015; 161:1453–1467. [PubMed: 26046444]

Thurman RE, Rynes E, Humbert R, Vierstra J, Maurano MT, Haugen E, Sheffield NC, Stergachis AB, Wang H, Vernot B, et al. The accessible chromatin landscape of the human genome. Nature. 2012; 489:75–82. [PubMed: 22955617]

Tiedemann RL, Putiri EL, Lee JH, Hlady RA, Kashiwagi K, Ordog T, Zhang Z, Liu C, Choi JH, Robertson KD. Acute depletion redefines the division of labor among DNA methyltransferases in methylating the human genome. Cell Rep. 2014; 9:1554–1566. [PubMed: 25453758]

Viré E, Brenner C, Deplus R, Blanchon L, Fraga M, Didelot C, Morey L, Van Eynde A, Bernard D, Vanderwinden JM, et al. The Polycomb group protein EZH2 directly controls DNA methylation. Nature. 2006; 439:871–874. [PubMed: 16357870]

Wani AH, Boettiger AN, Schorderet P, Ergun A, Münger C, Sadreyev RI, Zhuang X, Kingston RE, Francis NJ. Chromatin topology is coupled to Polycomb group protein subnuclear organization. Nat Commun. 2016; 7:10291. [PubMed: 26759081]

Weber M, Hellmann I, Stadler MB, Ramos L, Pääbo S, Rebhan M, Schübeler D. Distribution, silencing potential and evolutionary impact of promoter DNA methylation in the human genome. Nat Genet. 2007; 39:457–466. [PubMed: 17334365]

Wu H, Coskun V, Tao J, Xie W, Ge W, Yoshikawa K, Li E, Zhang Y, Sun YE. Dnmt3a-dependent nonpromoter DNA methylation facilitates transcription of neurogenic genes. Science. 2010; 329:444–448. [PubMed: 20651149]

Xie W, Schultz MD, Lister R, Hou Z, Rajagopal N, Ray P, Whitaker JW, Tian S, Hawkins RD, Leung D, et al. Epigenomic analysis of multilineage differentiation of human embryonic stem cells. Cell. 2013; 153:1134–1148. [PubMed: 23664764]

Yoon HG, Chan DW, Reynolds AB, Qin J, Wong J. N-CoR mediates DNA methylation-dependent repression through a methyl CpG binding protein Kaiso. Mol Cell. 2003; 12:723–734. [PubMed: 14527417]

Zentner GE, Tesar PJ, Scacheri PC. Epigenetic signatures distinguish multiple classes of enhancers with distinct cellular functions. Genome Res. 2011; 21:1273–1283. [PubMed: 21632746]

Zhang Y, Jurkowska R, Soeroes S, Rajavelu A, Dhayalan A, Bock I, Rathert P, Brandt O, Reinhardt R, Fischle W, Jeltsch A. Chromatin methylation activity of Dnmt3a and Dnmt3a/3L is guided by interaction of the ADD domain with the histone H3 tail. Nucleic Acids Res. 2010; 38:4246–4253. [PubMed: 20223770]

Ziller MJ, Gu H, Müller F, Donaghey J, Tsai LTY, Kohlbacher O, De Jager PL, Rosen ED, Bennett DA, Bernstein BE, et al. Charting a dynamic DNA methylation landscape of the human genome. Nature. 2013; 500:477–481. [PubMed: 23925113]

Highlights

- DNA methylation reversibly regulates H3K27me3 and H3K27ac at both promoters and enhancers
- H3K27me3 regulation by DNA methylation differs between bivalent and silent promoters
- Regulation of H3K27me3 is dependent on 5mC and requires DNMT catalytic activity

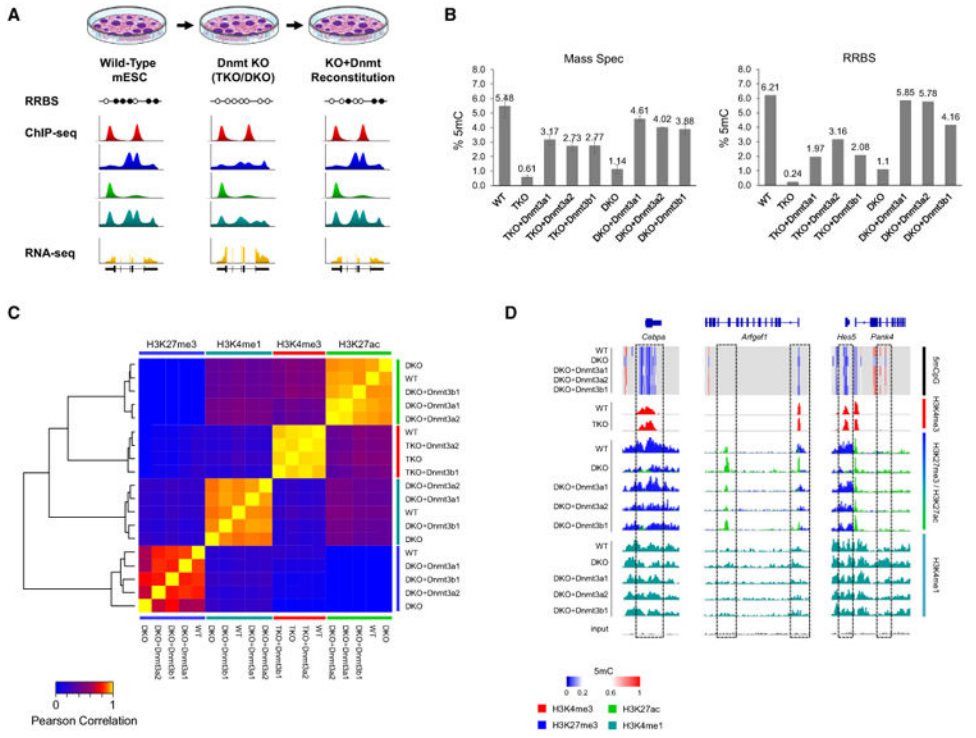

Figure 1. Alterations of DNA Methylation Cause Selective Genome-wide Changes in Histone Modifications

(A) Schematic of experimental design. Wild-type, TKO, DKO, and *Dnmt* Reconstitution cell lines each are assayed for DNA methylation by RRBS, histone modifications by ChIP-seq, and gene expression using RNA-seq.

(B) Left: mass spectrometry measurement of global 5mC levels between WT (n = 6), TKO (n = 7), TKO+*Dnmt3a1* (n = 5), TKO+*Dnmt3a2* (n = 6), TKO+*Dnmt3b1* (n = 4), and DKO and reconstitution cell lines (n = 2). Data are represented as mean ± SEM. Right: global 5mC levels measured by RRBS.

(C) Global Pearson correlation analysis between H3K27me3, H3K4me1, H3K4me3, and H3K27ac histone modifications across mESC lines. Correlation was calculated based on 1 kb genome-wide bins.

(D) Genome browser tracks of RRBS and histone modification ChIP-seq between WT, KO, and *Dnmt* reconstitution mESC lines. Regions of interest exhibiting histone modification changes are boxed.

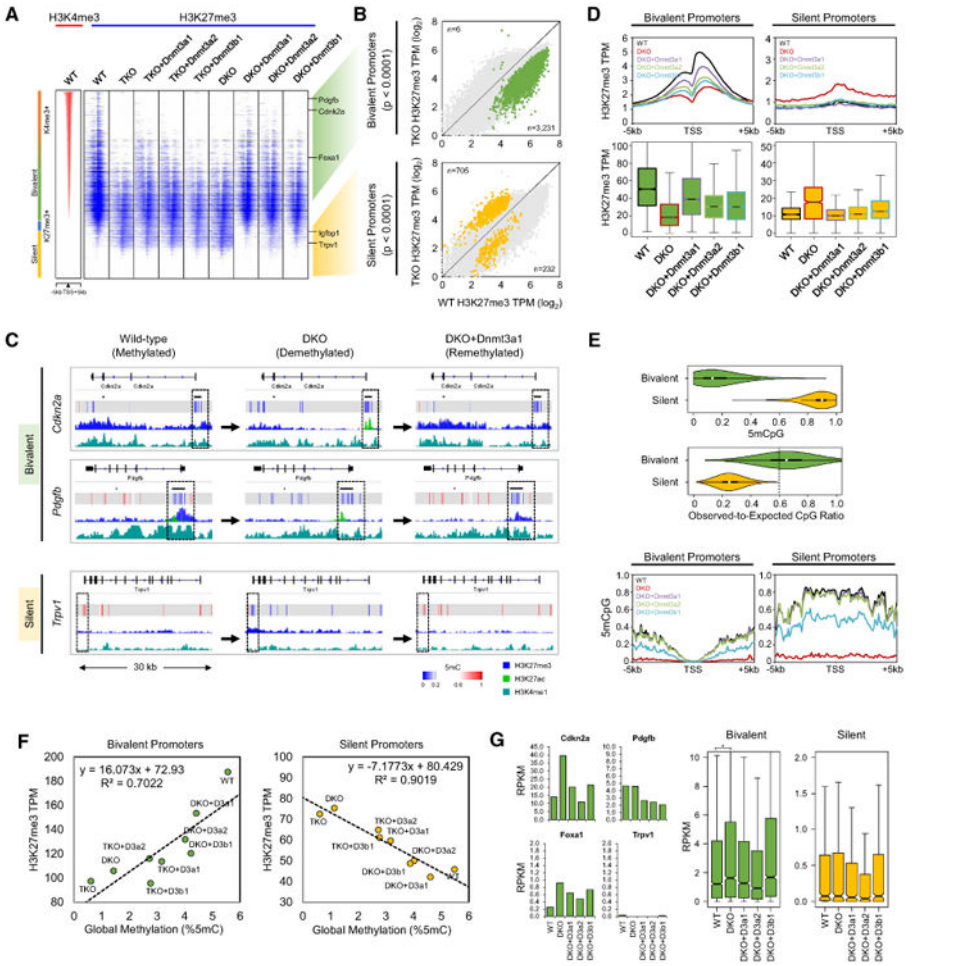

Figure 2. DNA Methylation Causally Regulates the Maintenance and Establishment of Promoter H3K27me3

(A) Heatmap of H3K4me3 (red) and H3K27me3 (blue) at ±5 kb region centered around all Refseq TSS ranked by H3K4me3. Promoter categories are shown on left. Representative genes from bivalent and silent promoter categories are shown on the right.

(B) Comparison of H3K27me3 between TKO versus WT at bivalent (top) and silent (bottom) promoters. Gray dots include all promoters and colored dots are statistically different between TKO and WT ($p < 0.0001$). Data are represented as H3K27me3 read coverage in log-transformed tags per 10 million (TPM) reads within 2 kb surrounding TSS of individual promoters.

(C) Genome browser tracks showing gene model, CpG islands, RRBS DNA methylation, H3K27me3/H3K27ac, and H3K4me1 (from top to bottom) at different loci. Promoter regions of *Cdkn2a* and *Pdgfb* (bivalent) and *Trpv1* (silent) are shown boxed.

(D) H3K27me3 occupancy in WT, demethylated DKO, and remethylated *Dnmt* reconstitution lines. Promoter metaplot and boxplot quantification of H3K27me3 occupancy between cell lines for bivalent (left) and silent (right) promoters. Metaplot represented as normalized H3K27me3 reads (in tags per 10 million; TPM) measured in 100 bp bins across ±5 kb centered at TSS. Boxplot data are similarly represented as H3K27me3 TPM within 2 kb surrounding TSS.

(E) Comparison of fractional CpG methylation and observed-to-expected CpG ratio between bivalent and silent promoters in 2 kb surrounding TSS (top). Promoter metaplot showing average CpG methylation at ±5 kb region centered around TSS (bottom).
(F) Promoter H3K27me3 correlates with global DNA methylation (measured by mass spec) at bivalent and silent promoters. Data are represented as normalized H3K27me3 in TPM within 5 kb of promoters and global 5mC (as in Figure 1B) are shown for each cell line. H3K27me3 TPM represents an average across all bivalent and silent promoters respectively. Note that the y axis scale is different between bivalent and silent promoters.
(G) Reads per kilobase million reads (RPKM) expression values for individual genes (left) and all bivalent and silent promoters (right). Bivalent promoters are expressed at a higher level in DKO relative to WT ($p = 4.75 \times 10^{-7}$, Kolmogorov-Smirnov test).

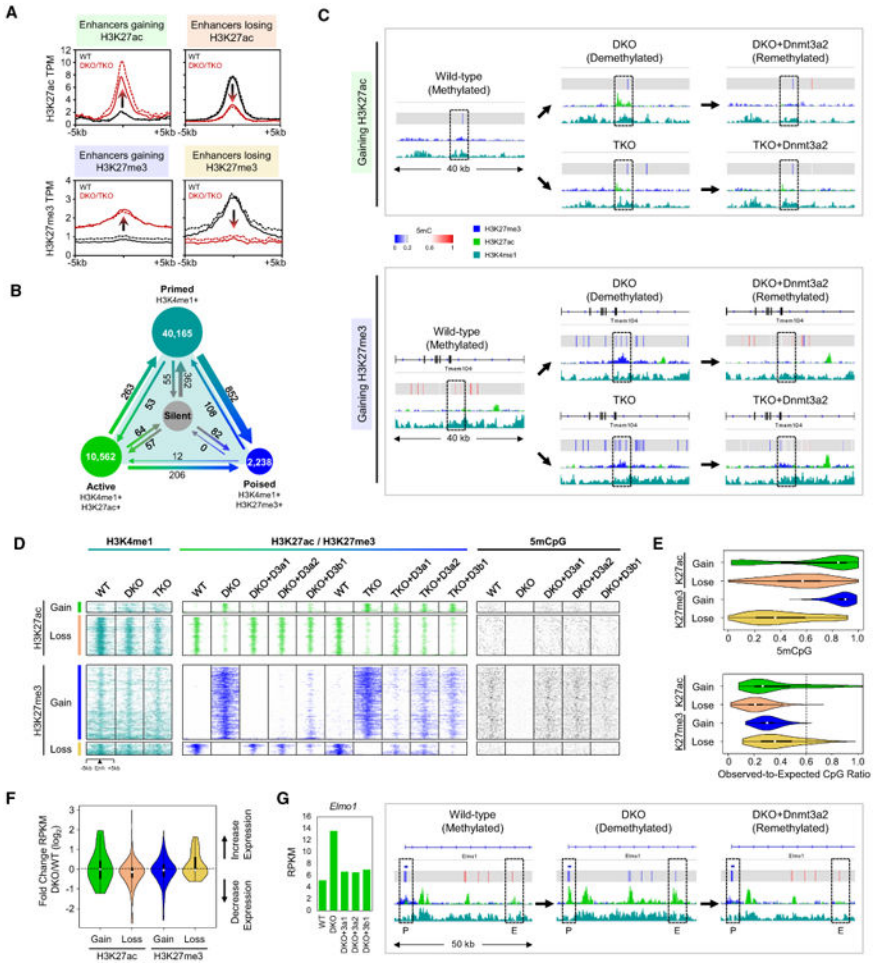

Figure 3. DNA Methylation Regulates Histone Modifications and Active States at Enhancers

(A) Altered histone modification occupancy at putative enhancer sites. Metaplot indicates H3K27ac and H3K27me3 read coverage from DKO (solid) and TKO (dashed), normalized by depth in 100 bp bins within ±5 kb around non-promoter H3K4me1 peaks.

(B) Schematic showing changes in candidate enhancer status between primed (H3K4me1$^+$), active (H3K4me1$^+$/H3K27ac$^+$), and poised(H3K4me1$^+$/H3K27me3$^+$) states. Numbers in circles indicate number of sites in WT mESC. Arrows represent changes occurring with demethylation in DKO/TKO.

(C) Genome browser visualization of histone modification changes at candidate de novo active (chr4:99,210,711-99,257,661; 80 kb upstream of *Foxd3*) and poised (chr11:115,049,693-115,089,693; *Tmem104* intragenic) enhancer sites.

(D) Heatmap analysis of histone modification changes to *Dnmt* DKO/TKO and reconstitution. Heatmap shows H3K4me1, H3K27ac, H3K27me3, and 5mCpG ±5 kb genomic region centered on H3K4me1 separated by candidate enhancer categories: H3K27ac gain (n = 138), H3K27ac loss (n = 551), H3K27me3 gain (n = 1,041), H3K27me3 loss (n = 162).

(E) Comparison of fractional CpG methylation (top) and observed-to-expected CpG ratio (bottom) in 2 kb surrounding enhancer center between categories of DNA methylation-sensitive enhancers.

(F) Distribution of log2 fold change (DKO/WT) in gene expression (in RPKM) between enhancer categories.

(G) Representative example of gene expression changes at *Elmo1* (chr13:20,175,630-20,231,247) showing increase in H3K27ac at intronic enhancer (boxed and labeled with E) and expression in DKO and reversion with *Dnmt* reconstitution.

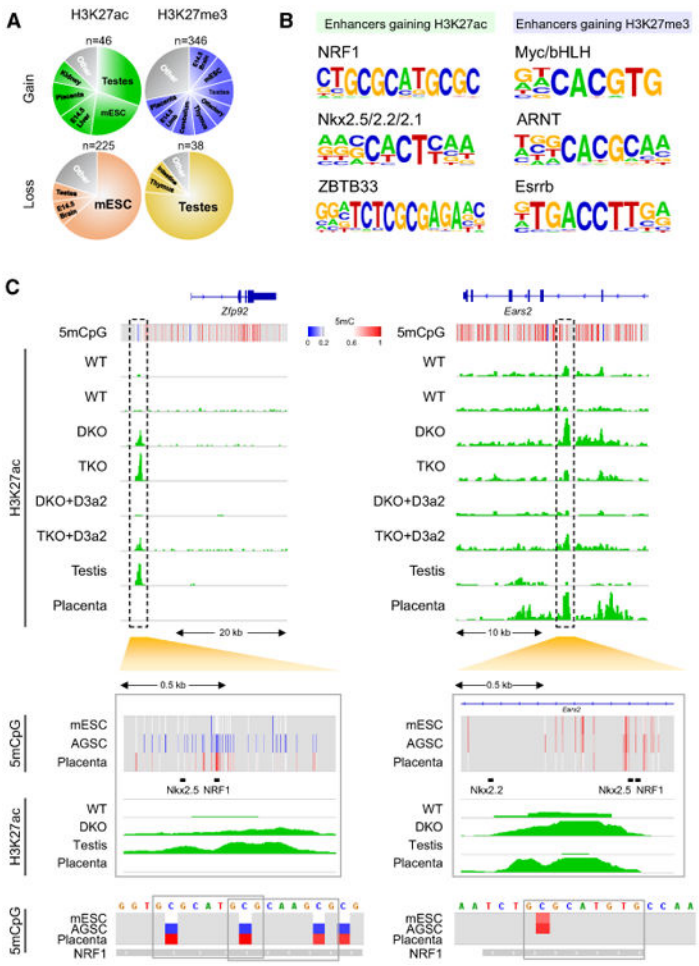

Figure 4. DNA Methylation Sensitive Regulatory Elements Include Both Tissue-Specific Promoters and Enhancers

(A) Candidate enhancers gaining or losing H3K27ac/me3 upon DNA demethylation are cross-referenced to previously identified tissue-specific enhancers (Shen et al., 2012). Tissues with candidate enhancer overlap >4% are labeled, and all remaining tissues are grouped in “Other” category.

(B) DNA sequence motifs enriched in de novo DNA methylation-dependent active and poised enhancer categories.

(C) Examples of tissue-specific enhancers overlapping differentially methylated regions and methylation-dependent transcription factor motifs enriched in our analysis. Genome browser tracks show enhancers upstream of *Zfp92* (chrX:70,622,988–70,673,292) and intragenic to *Ears2* (chr7:129,179,862–129,202,881). Whole-genome bisulfite sequencing tracks are shown for mESC, adult germline stem cell (AGSC) from testis, and placenta (Stadler et al., 2011; Hammoud et al., 2014; Hon et al., 2013).

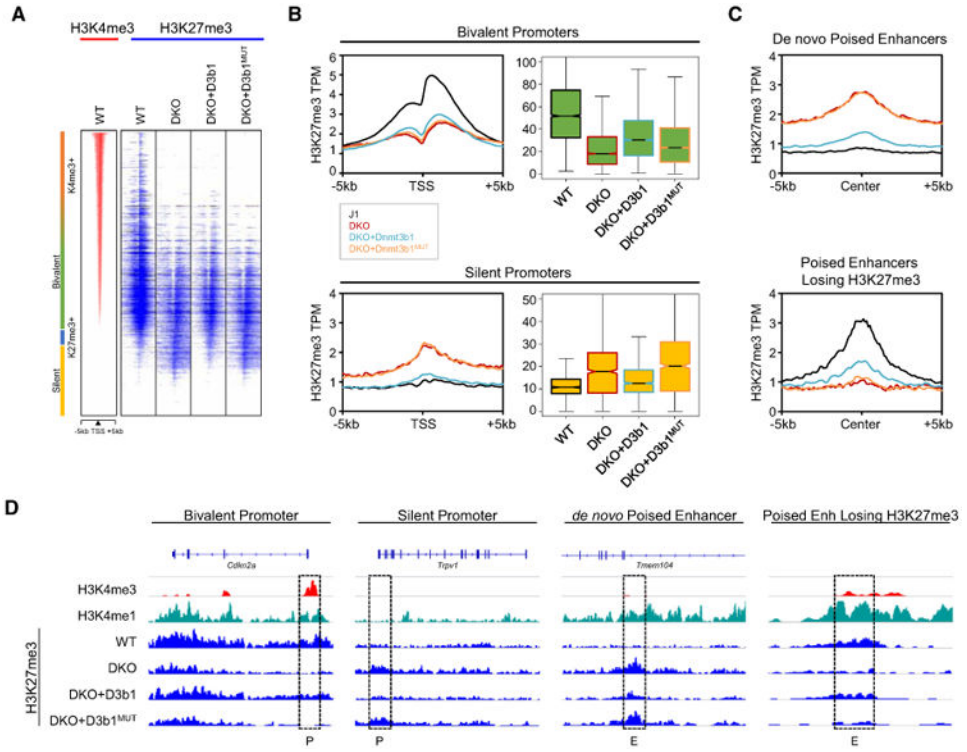

Figure 5. Regulation of H3K27me3 Depends on DNMT Catalytic Activity

(A) Heatmap of H3K4me3 (red) and H3K27me3 (blue) at ±5 kb region centered around all Refseq TSS ranked by H3K4me3. H3K27me3 compared between DKO, DKO+*Dnmt3b1* (wild-type), and DKO+*Dnmt3b1*^{MUT} (catalytic mutant).

(B) Comparison of H3K27me3 occupancy between wild-type *Dnmt3b1* and catalytic mutant reconstitution at bivalent and silent promoters. Average profile of H3K27me3 across ±5 kb centered on TSS and quantification between cell lines shown for bivalent (top) and silent promoters (bottom).

(C) Comparison between reconstitution of wild-type *Dnmt3b1* and *Dnmt3b1*^{MUT} at enhancers. Metaplot showing average profiles of H3K27me3 occupancy centered on de novo poised enhancers (top) and poised enhancers losing H3K27me3 (bottom).

(D) Genome browser tracks showing examples of H3K27me3 changes at promoters of *Cdkn2a* and *Trpv1* as well as de novo poised enhancer in Tmem104 and poised enhancer upstream of *Foxp4* (chr17:48,106,091–48,116,091).

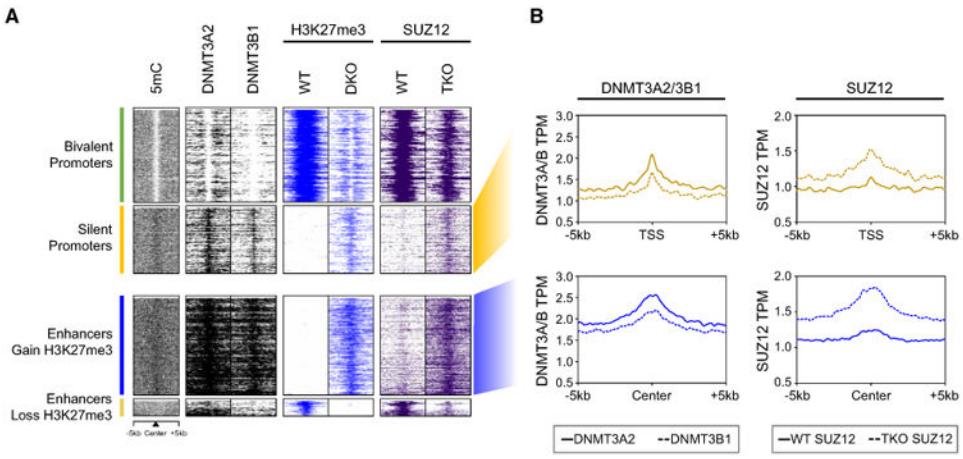

Figure 6. DNA Methylation Directly Regulates Loci Gaining H3K27me3 via PRC2 Occupancy

(A) Heatmap comparison of 5mC, DNMT3A2/B1, H3K27me3, and SUZ12 between different genomic contexts. Data are shown within ±5 kb centered on TSS or center of enhancer and quantified as averaged depth-normalized tags in 100 bp bins.

(B) Metaplot profiles showing average occupancy of DNMT3A2/3B1 and SUZ12 across silent promoters (top) and de novo poised enhancers (bottom) (Baubec et al., 2015; Cooper et al., 2014).

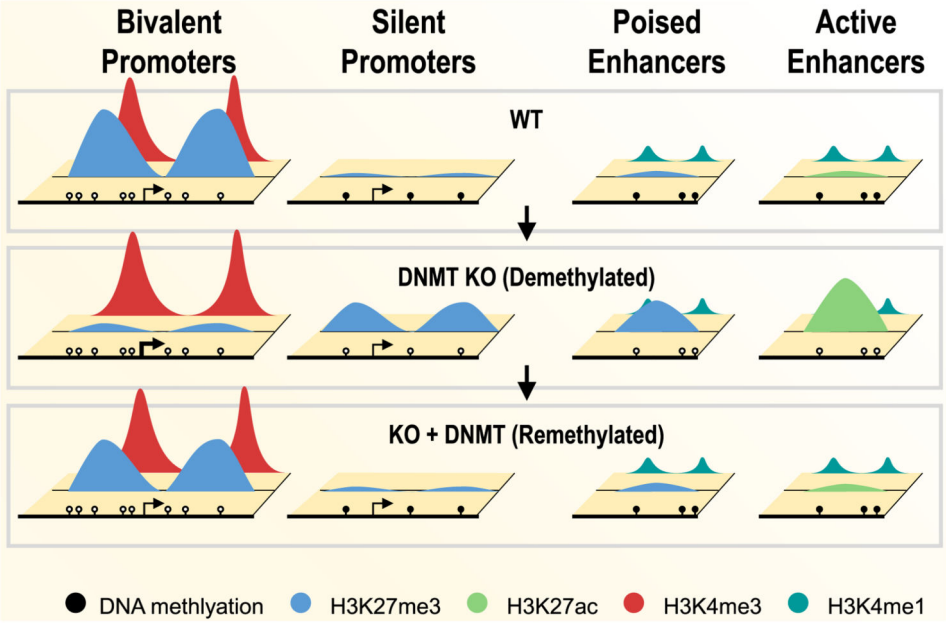

Figure 7. DNA Methylation Reversibly Regulates Histone Modifications across Promoter and Enhancer Contexts

Schematic of DNA methylation shaping of the epigenome. At promoters (left) hypomethylation results in loss or gain of H3K27me3, but not H3K4me3. Loss/gain of H3K27me3 is associated with H3K4me3 occupancy, where bivalent promoters marked by both H3K4me3 and H3K27me3 lose H3K27me3 with hypomethylation, while silent promoters absent of histone modifications gain H3K27me3 in the demethylated state. At enhancers (right) methylation represses enhancers, which become poised (gain H3K27me3) or active (gain H3K27ac) upon global demethylation. Reconstitution of DNMT in all contexts re-establishes WT patterns.